Near-threshold properties of the electronic density of layered quantum dots

Alejandro Ferrón,[1,*] Pablo Serra,[2,†] and Omar Osenda[2,‡]

[1]*Instituto de Modelado e Innovación Tecnológica (CONICET-UNNE), Avenida Libertad 5400, W3404AAS Corrientes, Argentina*

[2]*Facultad de Matemática, Astronomía y Física, Universidad Nacional de Córdoba and IFEG-CONICET, Ciudad Universitaria, X5016LAE Córdoba, Argentina*

(Received 28 December 2011; revised manuscript received 4 April 2012; published 25 April 2012)

We present a way to manipulate an electron trapped in a layered quantum dot based on near-threshold properties of one-body potentials. First, we show that potentials with a simple global parameter allow the manipulation of the wave function, changing its spatial localization. This phenomenon seems to be fairly general and could be implemented using current quantum-dot quantum-well technologies and materials if a proper layered quantum dot is designed. So, we propose a model layered quantum dot that consists of a spherical core surrounded by successive layers of different materials. The number of layers and the constituent materials are chosen to highlight the near-threshold properties. The manipulation of the spatial localization of the electron in a layered quantum dot yields results consistent with actual experimental parameters.

DOI: 10.1103/PhysRevB.85.165322 PACS number(s): 73.22.−f

I. INTRODUCTION

The tailoring of particular quantum states has become a usual task in quantum information processing.[1] Semiconductor quantum dots (QDs) are ideally suited to store quantum information through their eigenstates, since electrons in QDs can store quantum phase coherence for very long periods of time.[2] In addition, the amount of entanglement that a multielectron QD can keep in storage could be useful for implementing quantum information tasks, but there exist very few examples of *ab initio* calculations that attempt to quantify it in the literature.[3–8] The dots can be designed in a host of ways to meet the specific requirements of the quantum information task in sight, by choosing their shape, size, or materials.[9]

On the other hand, advances in semiconductor technology allow the preparation of more complex structures than the simple quantum well. Among the more complex structures, quantum-dot quantum-well structures[10] and multiple quantum rings[11] have been extensively studied. Quantum-dot quantum-well (QDQW) structures are multi-layered quantum dots composed of two semiconductor materials; the one with the smaller bulk band gap is sandwiched between a core and an outer shell of the material with larger bulk band gap. Because of their properties, QDQWs have been demonstrated to form an efficient gain medium for nanocrystal-based lasers,[12] and their electronic structure has been obtained from first-principles calculations.[13] It is remarkable that the effective mass approximation (EMA) seems to predict fairly well the behavior of the electronic density[13–15] when compared with first-principles calculations.

Quantum ring structures are an ideal playground to study many subtle quantum phenomena such as the Aharonov-Bohm effect,[16] which leads to the presence of persistent currents.[17] These persistent currents have been measured even for one-electron states.[18] Quantum rings are formed by only one semiconductor material, and the fabrication of multiple concentric quantum rings (up to five) can be achieved with high quality and reliability.[19]

Despite all the advantages that quantum dots present as implementations of physical qubits, the confined electrons interact with thousands of spin nuclei through the hyperfine interaction. This leads, inevitably, to decoherence. To solve the decoherence problem it has been proposed that the physical qubit should be implemented by two electrons confined in a double quantum dot.[20] The coupling of the two quantum dots depends on the spatial extent of the one-electron wave functions; in particular it determines the strength of the exchange interaction between the two electrons. The exchange coupling in double quantum dots has been studied extensively, with particular focus on how it can be tuned using electric fields,[21] magnetic fields,[22] or the effect of the confinement of the double quantum dot in a quantum wire.[23] So, the ability to manipulate the spatial extent of the one-electron wave function in an isolated QD can be decisive when dealing with the states of a double quantum dot.

In addition, recent advances in materials manipulation at the nanoscale level allow accurate shape and size control of the QD, which offers the possibility of tailoring the energy spectrum to produce desirable optical transitions. These tasks are useful for the development of optical devices with tunable emission or transmission properties. Optical properties of artificial molecules and atoms are subjects of great interest because of their technological implementations. In spherical QDs, optical properties such as the dipole transition, the oscillator strength, and the photoionization cross section have been studied theoretically by different authors.[24–29]

In this work we present a way to manipulate the wave function of an electron trapped in a quantum dot whose energy is near the continuous threshold. The phenomena associated seem to be fairly general and could be implemented using current quantum-dot quantum-well technologies and materials. In particular, we show that the phenomenon is present in a layered quantum dot model whose parameters are consistent with actual experimental values.

The paper is organized as follows. In Sec. II we introduce a simple model whose near-threshold behavior shows how the localization of the ground-state electronic density could be handled easily. In Sec. III we apply the findings of Sec. II to design a QDQW-like model that is both consistent with actual experimental values and able to exploit the near-threshold phenomenon. Here we perform calculations for the ground

state and the first excited p state, and we analyze the optical properties of the model. Finally, Sec. IV contains the conclusions, with a discussion of the most relevant points of our findings.

II. ONE-ELECTRON OSCILLATING POTENTIAL

In this section we report results for the ground-state electronic density of one electron in an oscillating short-range potential. We choose a smooth and analytical potential to emphasize that the behavior of the electronic density is fairly general. The near-threshold properties will be exploited in the next section to design quantum-dot structures modeled by steplike potentials.

The one-particle Hamiltonian is given by

$$H = -\frac{\hbar^2}{2m}\nabla^2 + W(r), \tag{1}$$

where

$$W(r) = -W_0 e^{-\gamma r}\sin(\omega r), \tag{2}$$

and where W_0 is the strength of the potential and γ and ω are positive constants. Clearly, the potential-well range is given by γ, and the number of spherical layers and their widths are related to ω. The successive spherical layers are similar to a succession of potential wells and barriers.

It is known that, for fixed values of γ and ω, there is a critical value $W_0^{(c)}$ such that the Hamiltonian in Eq. (1) supports at least one bound state only if $W_0 > W_0^{(c)}$.[30] In the following, we will study the near-threshold properties of the ground-state electronic density varying W_0 as a global parameter, for $W_0 \gtrsim W_0^{(c)}$.

The ground-state energy and wave function of the Hamiltonian in Eq. (1) were obtained numerically using the fourth-order Runge-Kutta method for the potential in Eq. (2). The electronic density $\rho(r)$ is given by

$$\rho(r) = \int |\Psi(\mathbf{r})|^2 r^2\, d\Omega, \tag{3}$$

where Ψ is the one-electron wave function. We are interested in the probability of finding the electron in the nth well. Figure 1 shows the electronic density $\rho(r)$ for different values of W_0. By changing the value of W_0 it is possible to select the potential well in which the maximum value of the electronic density is located. The particular value of W_0 that locates the maximum of the electronic density in, say, the third well depends on the actual values of γ and ω.

In Fig. 2(a) we can observe the position where the electronic density achieves its maximum value ($r_{\max}$). We can check that the value $r_{\max}$ is rather stable as a function of W_0. Moreover, Fig. 2(a) shows that changing W_0 allows selection of the well in which the electronic density will have its maximum value. It is worth mentioning that this effect is a near-threshold phenomenon different from those reported previously in the literature for electrons localized in complex nanostructures,[10,22] since in our example the maximum is not necessarily located in the deepest well.

The maximum in the electronic density as a function of the strength potential shows an interesting phenomenon. We can observe how this maximum jumps from a well to the next well when the strength potential is continuously varied. It is important to note that we have a situation where the maximum is not located in the deepest well. In order to clarify this phenomenon we define the "well occupation probability,"

$$I_n = \int_{2(n-1)\pi/\omega}^{(2n-1)\pi/\omega} \rho(r)dr, \tag{4}$$

which allows us to evaluate how much of the electronic density is in the nth well. In Fig. 2(b) we show the numerical calculations of I_n for different values of n. The intersection of the black solid line (I_1) and the red dashed line (I_2) of Fig. 2(b) gives us the value of W_0 where a qualitative change in the electronic density occurs. For this value of W_0 we have the first jump. The second jump occurs for the value of W_0 where the red dashed line and the blue dash-dotted line intersect.

Finally, in Fig. 3 we plot the contour map of the electronic density as a function of the coordinate r and the strength potential W_0 for the potential defined in Eq. (2). Here we can appreciate clearly the effect reported in this work. For larger values of W_0 ($W_0 > 0.25$) the electronic density presents just one peak located in the first well. When we decrease the value of W_0 we start to see a second (lower) peak located in the second well, but for values of $W_0 \simeq 0.2$ the second peak is higher than the first peak and the maximum is not located in the deepest well. If we continue decreasing W_0 the peak in the first well vanishes and we start to appreciate a new peak in the third well.

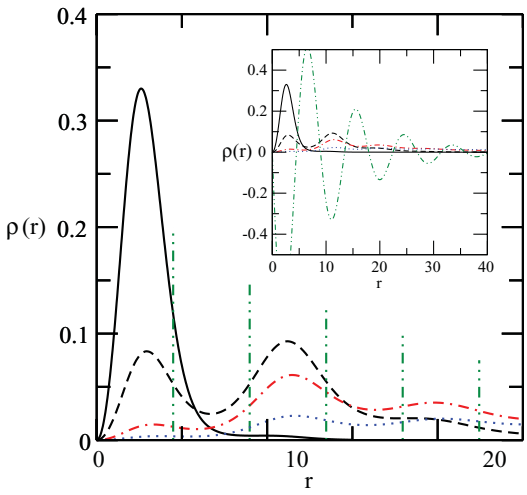

FIG. 1. (Color online) Electronic density as a function of r for the ground-state Hamiltonian [Eq. (1)]. The dark green vertical dash-dotted lines show the zeros of the potential defined in Eq. (2). The black continuous line shows the electronic density for $W_0 = 0.3$ a.u., the black dashed line shows the electronic density for $W_0 = 0.2$ a.u., red dash-dotted line shows the calculation for $W_0 = 0.16$ a.u., and the blue dotted line shows the electronic density for $W_0 = 0.14$ a.u. The inset shows the same electronic densities and the potential at a different scale. The dark green dash-dotted curve corresponds to the potential, which is plotted in W_0 units.

III. ONE-ELECTRON QDQW-LIKE MODEL

The ability to produce easily distinguishable quantum states in nanodevices is of fundamental importance because of its potential technological applications, so we show that the

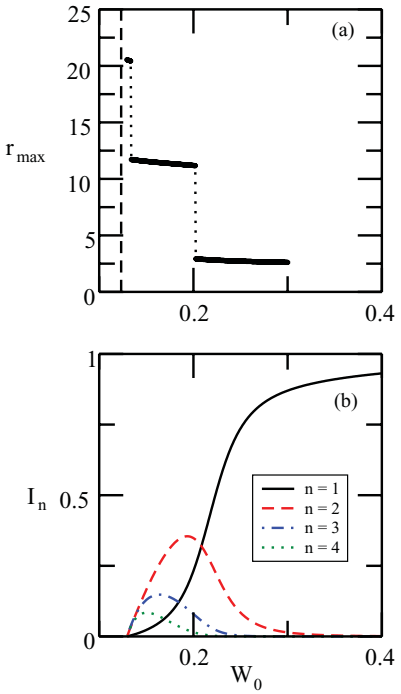

FIG. 2. (Color online) (a) Position where the electronic density achieves its maximum value (r_{max}) as a function of W_0. The vertical dashed line shows the critical ionization value $W_0^{(c)}$. (b) The well occupation probability I_n as a function of W_0. For large values of W_0 the ground state wave function is localized around the origin, so only I_1 is appreciable. For smaller values of W_0, I_1 drops to zero and the successive wells became occupied. Near the threshold many wells are occupied but $I_n \to 0$, $\forall n$.

spatial extent of the ground-state electronic density can be noticeably changed without changing the spatial extent of the nanostructure. The ground states could be distinguished by current imaging techniques.[31]

In the following we show how our findings could be relevant in actual physical implementations. The synthesis of layered quantum dots is a well known technique; see Ref. 10 and references therein. Moreover, the EMA approximation appropriately describes the electronic structure of nanostructures formed by layers of CdS and HgS. Since the modulation of a global parameter such as our W_0 is not easily achievable, and since the potential well in CdS/HgS compounds is given by the conduction-band offset between the two materials, the only parameters that can be varied with some ease by experimentalists are the widths and the materials of the layers. Another difference when dealing with heterogeneous nanostructures with the simple model Hamiltonian in Eq. (1) results from the different effective-mass characteristic of each material.

Here we consider structures with two wells made of a HgS layer, separated by one CdS step and with a central CdS core. The steplike potential can be written

$$V(r) = \begin{cases} V_0, & r < r_c \quad \text{(CdS)}, \\ 0, & r_c \leqslant r < r_1 \quad \text{(HgS)}, \\ V_0, & r_1 \leqslant r < r_2 \quad \text{(CdS)}, \\ 0, & r_2 \leqslant r < r_3 \quad \text{(HgS)}, \\ V_0, & r \geqslant r_3 \quad \text{(CdS)}, \end{cases} \tag{5}$$

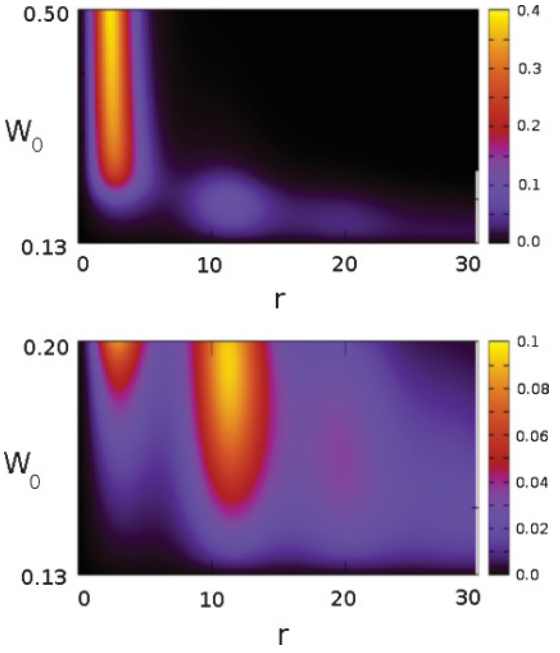

FIG. 3. (Color online) The upper panel shows the contour map of the electronic density as a function of the coordinate r and the strength potential W_0 for the potential defined in Eq. (2). A zoom of this figure is shown in the lower panel. The figures show how the electronic density's higher peak moves as W_0 decreases. Note that for certain values of W_0 the electronic density has one, two, or three peaks.

where the potentialwell depth is $V_0 = 1.35$ eV, which corresponds to the band offset between CdS and HgS, while the effective masses are $0.2m_e$ and $0.036m_e$ respectively.[32] The widths of the inner and outer HgS layers were fixed equal to 2 and 1.5 nm, respectively, while the width of CdS layer that separates them was fixed to 2 nm. The width of the central CdS core is going to be varied in order to show the phenomenon presented in the previous section. An important difference with W_0 is that the width of the layers can be varied easily in the laboratory.

A. Ground-state electronic density

Here we evaluate the ground-state electronic density for the layered QD given by Eq. (5), as we did in the previous section.

As Fig. 4 shows, by changing the width of the CdS core the electronic density maximum can be located in the potential well of choice. In addition, the position of the maximum, as a function of the core width, shows the same behavior as the electronic density of the model Hamiltonian; compare Figs. 4(c) and 2(a).

The stability of the electronic density's maximum can be used when dealing with coupled structures. The fabrication of nanodevices is subject to many errors, so at least in principle it could be very useful to have nanostructures whose properties are not excessively sensitive to the actual fabrication parameters.

B. Optical properties

Optical properties are related to the transitions between different states of the quantum system. In this section we

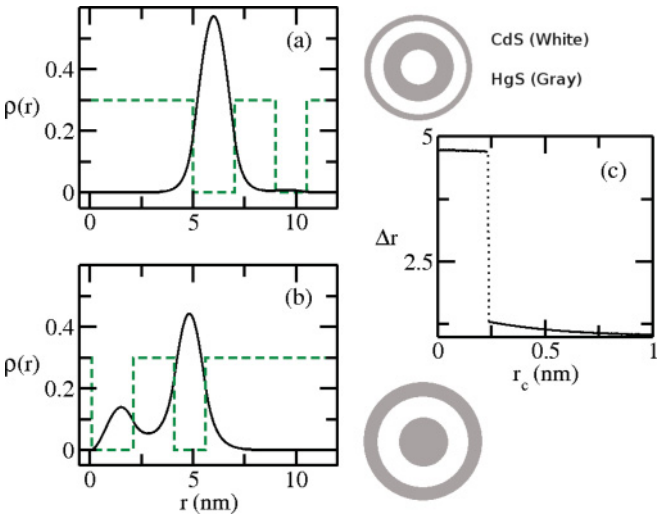

FIG. 4. (Color online) The electronic density for two different layered quantum dots. The electronic density in panel (a) corresponds to a CdS/HgS/CdS/HgS/CdS structure ($r_c = 2$ nm), while panel (b) corresponds to a HgS/CdS/HgS/CdS one ($r_c = 0$ nm). The structures are shown as ring patterns (after the last HgS layer we consider that we have a very long CdS barrier). Panel (c) shows the behavior of the position where the electronic density achieves its maximum value ($\Delta r = r_{\max} - r_c$), measured with respect to the inner radius of the first potential well as a function of the core width r_c. For large enough values of the CdS core the electronic density maximum lies in the first potential well, as shown in panel (a). When the radius of the CdS core approaches 0.5 nm the maximum of the electronic density jumps to the second potential well, as shown by the abrupt change in Δr in panel (c). The green dashed line in (a) and (b) shows the steplike potential.

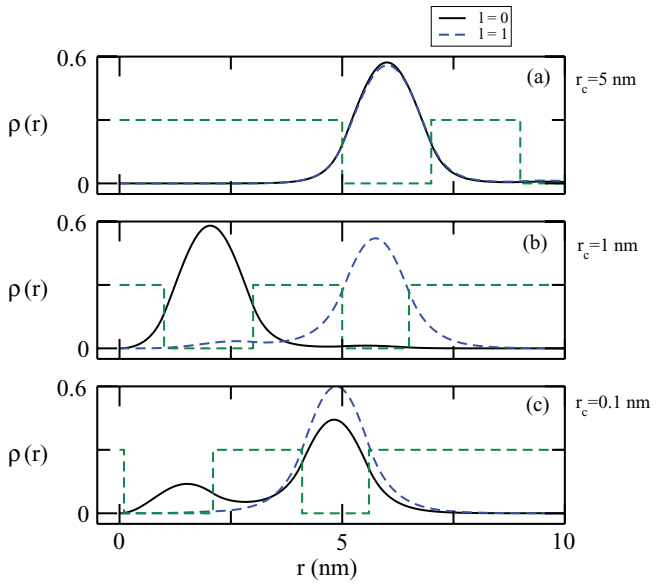

FIG. 5. (Color online) The electronic density for three different CdS/HgS/CdS/HgS/CdS layered quantum dots. The electronic density in panel (a) corresponds to $r_c = 5$ nm, while for panel (b) $r_c = 1$ nm and panel (c) $r_c = 0.1$ nm. The dark green dashed line in (a), (b), and (c) shows the steplike potential.

need to evaluate the ground state and some of the excited states of the one-electron system. As we mentioned before, the phenomenon under investigation is a near-threshold property of the system; because of that, the calculation of the excited states requires some effort.

In Fig. 5 we show the electronic densities for the ground state and the lower excited state with angular momentum $l = 1$. In Fig. 5(a) we can see that the maxima of both electronic densities are located in the first potential well. As we decrease the width of the central core (r_c) we observe that the maximum value of the excited-state electronic density jumps to the second potential well, while the ground-state electronic density remains almost unchanged [Fig. 5(b)]. Finally, for small values of the central CdS core we obtain the picture presented before. In Fig. 5(c) we can see that the maxima of both electronic densities ($l = 0$ and $l = 1$) are located in the second potential well. It is reasonable to assume that this issue must be reflected in the transition rates between these states, and therefore in the optical properties of the one-electron QDQW.

It is worth mentioning that the overlap between the ground state and the excited p state varies from almost 1 [see Fig. 5(a)] to a very small value [see Fig. 5(b)], and back [see Fig. 5(c)], without changing very much the size of the device. This feature cannot be achieved with a single-well QD without changing its size over one or two orders of magnitude, since for very large QDs the eigenfunctions become very delocalized, resulting in a large overlap between them.

In order to analyze the optical properties of the one-electron layered quantum dots, we are going to investigate the electronic dipole-allowed transitions. For this purpose we calculate the oscillator strength P_{if}, which is a dimensionless quantity that can be evaluated using the expression[33]

$$P_{if} = C\Delta E_{fi}|M_{fi}|^2, \tag{6}$$

where M_{fi} is the dipole transition matrix element between the lower state (i) and the upper state (f), $\Delta E_{fi} = E_f - E_i$, and C is a normalization constant. Following the work of Buczko and Bassani,[33] we used the Thomas-Reiche-Kuhn sum rule,

$$\sum_n P_{0n} + \int_0^\infty P_{0E}\, dE = 1, \tag{7}$$

to calculate the normalization constant

$$C = \langle 0|\frac{1}{m^\star(r)}|0\rangle^{-1}, \tag{8}$$

where $|0\rangle$ is the ground-state ket and $m^\star(r)$ the steplike effective mass of the electron, $0.2m_e$ for CdS and $0.036m_e$ for HgS.

In Fig. 6(a) we can observe the oscillator strength for the transitions between the ground state and the lower excited state with $l = 1$, as a function of the core width. In the lower panel, Fig. 6(b), we show, as in Fig. 4(c), the behavior of the position where the electronic densities (ground and excited states) achieve their maximum values ($\Delta r = r_{\max} - r_c$), measured with respect to the inner radius of the first potential well as a function of the core width r_c. For large enough values of the CdS core, the electronic density maxima lie in the first potential well. As the radius of the CdS core decreases, the maxima

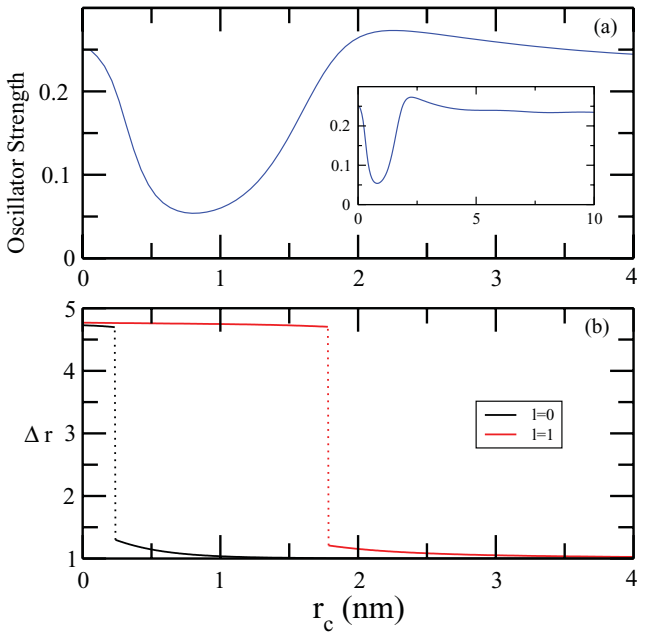

FIG. 6. (Color online) Panel (a) shows the oscillator strength as a function of the core width r_c calculated using Eq. (6) for the ground and lower excited states with $l = 1$. Panel (b) shows the behavior of the position where the electronic densities achieves their maximum values ($\Delta r = r_{\max} - r_c$), measured with respect to the inner radius of the first potential well as a function of the core width r_c. For large enough values of the CdS core the electronic density maxima lie in the first potential well. When the radius of the CdS core approaches 1.8 nm (0.23 nm) the maximum of the excited sate (ground state) electronic density jumps to the second potential well, as shown by the abrupt change in Δr.

of the electronic densities jump to the second potential well ($r_c = 1.8$ nm for the excited-state density and $r_c = 0.23$ nm for the ground-state density), as shown by the abrupt change in Δr. As we can see in the inset of Fig. 6(a), the oscillator strength rapidly decreases for large values of the width of the central CdS core and then reaches a limiting value. The behavior for small values of r_c is rather more complicated, and, as was pointed out before, the phenomenon becomes evident. It is clear from Figs. 6(a) and 6(b) that, when the maximum values of the electronic densities are located in different potential wells, the oscillator strength presents a dramatic decrease.

IV. CONCLUSIONS

We have shown a complete analysis of the ground state of one electron in a spherical potential described in Eqs. (2) and (5). For the potential defined in Eq. (5) we analyzed the ground and the lower excited states with $l = 1$. The effect mentioned before is also present in the excited state. We finished the present work with the study of the optical properties of one-electron layered quantum dots. Here we find that the effect is detected by the oscillator strength, which is a very important physical quantity in the study of the optical properties, and is related to electronic dipole-allowed transitions. Moreover, we conclude that we can have great control of the optical properties of these nanostructures in a simple manner using the well known techniques of synthesis of layered quantum dots. A small change in the width of the central core can produce dramatic changes in the optical properties of QDQWs.

This phenomenon can be experimentally observed with actual semiconductor technology. One possible setback for the observation of the phenomenon discussed in this work comes from the low binding energies associated with near-threshold phenomena. Given the fairly simple dependence of the reported phenomenon on the potential characteristics, we believe that its observation is possible and feasible. For the model analyzed in this paper, the availability of materials with larger band offsets could render the phenomenon more pronounced and with larger eigenenergies.

The behavior of the electronic density in one- and two-dimensional systems with a potential equivalent to Eq. (2) is qualitatively the same. Anyway, since the near-threshold behavior in two dimensions is not exactly the same as that observed in three dimensions, it is possible that the jump of the electronic density between two-dimensional potential wells could be observed more easily than in the three-dimensional case. On the other hand, since in near-threshold two-dimensional systems the wave function rapidly spreads over very large regions, a delicate trade-off between the localization and delocalization could take place.

Another possible extension of our problem, to be studied, is its appearance in electrostatic quantum dots.[34]

ACKNOWLEDGMENTS

We would like to acknowledge SECYT-UNC, CONICET, and MinCyT Córdoba for partial financial support of this project.

*aferron@conicet.gov.ar
†serra@famaf.unc.edu.ar
‡osenda@famaf.unc.edu.ar

[1] R. Brunner, Y.-S. Shin, T. Obata, M. Pioro-Ladrière, T. Kubo, K. Yoshida, T. Taniyama, Y. Tokura, and S. Tarucha, Phys. Rev. Lett. **107**, 146801 (2011).
[2] R. Takahashi, K. Kono, S. Tarucha, and K. Ono, Phys. Rev. Lett. **107**, 026602 (2011).
[3] A. Ferrón, O. Osenda, and P. Serra, Phys. Rev. A **79**, 032509 (2009).
[4] F. M. Pont, and O. Osenda, J. H. Toloza, and P. Serra, Phys. Rev. A **81**, 042518 (2010).
[5] F. M. Pont, O. Osenda, and P. Serra, Phys. Scr. **82**, 038104 (2010).
[6] M. Bylicki, W. Jaskólski, A. Stachów, and J. Diaz, Phys. Rev. B **72**, 075434 (2005).
[7] J. P. Coe and I. D'Amico, J. Phys.: Conf. Ser. **254**, 012010 (2010).
[8] S. Abdullah, J. P. Coe, and I. D'Amico, Phys. Rev. B **80**, 235302 (2009).
[9] S. M. Reimann and M. Manninen, Rev. Mod. Phys. **74**, 1283 (2002).
[10] D. Schooss, A. Mews, A. Eychmüller, and H. Weller, Phys. Rev. B **49**, 17072 (1994).
[11] T. Mano, T. Kuroda, S. Sanguinetti, T. Ochiai, T. Tateno, J. Kim, T. Noda, M. Kawabe, K. Sakoda, G. Kido, and N. Koguchi, Nano Lett. **5**, 425 (2005).

[12]J. Xu and M. Xiao, Appl. Phys. Lett. **87**, 173117 (2005).
[13]J. Schrier and L.-W. Wang, Phys. Rev. B **73**, 245332 (2006).
[14]J. Berezovsky, M. Ouyang, F. Meier, D. D. Awschalom, D. Battaglia, and X. Peng, Phys. Rev. B **71**, 081309(R) (2005).
[15]F. Meier and D. D. Awschalom, Phys. Rev. B **71**, 205315 (2005).
[16]M. Bayer, M. Korkusinski, P. Hawrylak, T. Gutbrod, M. Michel, and A. Forchel, Phys. Rev. Lett. **90**, 186801 (2003).
[17]D. Mailly, C. Chapelier, and A. Benoit, Phys. Rev. Lett. **70**, 2020 (1993).
[18]N. A. J. M. Kleemans, I. M. A. Bominaar-Silkens, V. M. Fomin, V. N. Gladilin, D. Granados, A. G. Taboada, J. M. García, P. Offermans, U. Zeitler, P. C. M. Christianen, J. C. Maan, J. T. Devreese, and P. M. Koenraad, Phys. Rev. Lett. **99**, 146808 (2007).
[19]C. Somaschini, S. Bietti, N. Koguchi, and S. Sanguinetti, Nano Lett. **9**, 3419 (2009).
[20]R. Petta, A. C. Johnson, J. M. Taylor, E. A. Laird, A. Yacoby, M. D. Lukin, C. M. Marcus, M. P. Hanson, and A. C. Gossard, Science **309**, 2180 (2005).
[21]A. Kwasniowski and J. Adamowski, J. Phys.: Condens. Matter **21**, 235601 (2009).
[22]B. Szafran, F. M. Peeters, and S. Bednarek, Phys. Rev. B **70**, 125310 (2004).
[23]L.-X. Zhang, D. V. Melnikov, S. Agarwal, and J.-P. Leburton, Phys. Rev. B **78**, 035418 (2008).
[24]J. L. Gondar and F. Comas, Physica B **322**, 413 (2003).
[25]S. Yilmaz and H. Safak, Physica E **36**, 40 (2007).
[26]A. Özmen, Y. Yakar, B. Cakir and Ü. Atav, Opt. Commun. **282**, 3999 (2009).
[27]J. S. deSousa, J. P. Leburton, V. N. Freire, and E. F. daSilva, Phys. Rev. B **72**, 155438 (2005).
[28]I. Karabulut and S. Baskoutas, J. Appl. Phys. **103**, 073512 (2008).
[29]M. Sahin, Phys. Rev. B **77**, 045317 (2008).
[30]S. Kais and P. Serra, Adv. Chem. Phys. **125**, 1 (2003).
[31]A. Patanè, N. Mori, O. Makarovsky, L. Eaves, M. L. Zambrano, J. C. Arce, L. Dickinson, and D. K. Maude, Phys. Rev. Lett. **105**, 236804 (2010).
[32]G. W. Bryant, Phys. Rev. B **52**, R16997 (1995).
[33]R. Buczko and F. Bassani, Phys. Rev. B **54**, 2667 (1996).
[34]S. Bednarek, B. Szafran, K. Lis, and J. Adamowski, Phys. Rev. B **68**, 155333 (2003).